Multicellular Pattern Formation

Parameter Estimation for Ordinary Differential Equation-Based Gene Regulatory Network Models

BY TIM HOHM
AND ECKART ZITZLER

Understanding the self-regulatory mechanisms controlling the spatial and temporal structure of multicellular organisms represents one of the major challenges in molecular biology. Although high-throughput data have become available with the advances in experimental technologies at a large scale, measuring gene expression levels at a high spatial resolution remains extremely difficult. As a result, the study of genetic regulatory networks in the light of spatial expression patterns still relies mainly on qualitative data. This leads to the question of how to fit the parameters of a gene regulatory network model such that a purely qualitatively defined pattern can be reproduced.

This article addresses this issue and presents a general approach to generate patterns reflecting basic geometric shapes. In combination with an appropriate ordinary differential equation (ODE)-based modeling and simulation framework, a formalism to quantify qualitative patterns and integrate this concept into an evolutionary algorithm for parameter estimation is presented and tested for stripe-like patterns on two test systems.

Patterns resulting from gene regulative events are pervasive in nature. Apart from easily observable patterns, e.g., animal coats, patterns are prevalent in many tissues [1], [2]. Understanding the formation and maintenance of such patterns goes hand in hand with understanding the gene regulation events. However, generating high-resolution spatial quantitative data preferentially used for the inference of the underlying regulative mechanisms proves to be a major challenge with respect to the experimental techniques. Nevertheless, quite detailed hypotheses about feedback mechanisms constituting the regulative networks are known, e.g., for the shoot apical meristem (SAM) of the plant *Arabidopsis thaliana* [2]. Such hypotheses resulting from various specific experiments can be subsumed to qualitative patterns formed by domains of high- or low-gene expressions, e.g., the organizing center and stem-cell domain in the SAM (see Figure 1).

Given such a qualitative picture of the tissues under consideration, the key question is how to use this information to test and develop refined hypotheses on the structure of gene-regulative networks (GRNs) responsible for producing the observed patterns. One of the steps involved in answering this question is to test whether a putative interaction network can reproduce a certain qualitative target pattern. For example, given a putative interaction network in the form of a system of ODEs, it needs to be checked if there exists a set of parameters for this model resulting in the target pattern. Since the target pattern is defined only qualitatively, quantifying the similarity between model output and the target pattern poses a difficult problem. In this article, we address this problem and present a parameter optimization technique for the described setup. In particular, we discuss the questions of how to formalize qualitative patterns and how to quantify similarity between patterns.

Digital Object Identifier 10.1109/MEMB.2009.932905

Related Work

The described problem of testing whether, given a putative GRN, there exists a parameter set leading to a specified desired system behavior is part of a GRN inference process: starting from an initial model, the model and model parameters are tuned in an iterative process to better explain the available data. Today, there exists a variety of different inference methods; an overview is given in [3]. Usually, for model fitting, they rely on quantitative data and often even time course data, a type of data only scarcely available for the considered multicell setups. Instead, most of the time, only qualitative data about systems' equilibrium states are available.

To date, only a few studies [4], [5] exist dealing with multicell setups for which only qualitative data are available: the focus of these studies is on hypothesis testing, but no exploration about the hypotheses has been performed so far; information gained during testing is only scarcely fed back to refine the original hypothesis. Therefore, to perform automated hypothesis exploration, the evaluation of the model fit has to be done in a computer-accessible way: 1) target patterns have to be described formally and 2) a quantitative measure for similarity between target pattern and simulated patterns is needed—two issues that are at the center of this study.

Quantification of Qualitative Patterns

The similarity quantification method developed in this article depends on the type of tissue representation. Therefore, before explaining the pattern identification and quantification procedure, we briefly describe the underlying modeling and simulation framework.

Understanding the formation and maintenance of such patterns goes hand in hand with understanding the gene regulation events.

Modeling and Simulation Framework

The tissue model explicitly represents all cells of the tissue while maintaining the spatial organization of the tissue. The building block of this model is a cell v. Each cell is characterized by a vector of gene-product concentrations or gene-expression levels. The spatial organization of the tissue is captured by internally representing the tissue as a graph $G(V, E)$, where V denotes the set of cells, and E is a set of directed edges, containing the edges $e_{i,j}$ and $e_{j,i}$ for all pairs of cells (v_i, v_j) sharing common cell surface.

This tissue representation is coupled with a model for system dynamics: an ODE GRN model. The ODEs describe the intracellular interactions between the genes and intercellular interactions between neighboring cells. The considered neighborhood $N(v_i)$ of a cell v_i is defined by the set of cells v_j for which $e_{i,j} \in E$ holds, and cell interaction between these cells are assumed to happen by diffusion of gene products between these cells.

The tissue behavior over time is then simulated by means of numerical integration of the ODEs. For a more detailed description of the used model, see [6].

Similarity Measure

Now, given a specification of a particular tissue using the aforementioned representation, the notion of a target pattern needs to be formalized, and the pattern components need to be identified in a given picture to quantify the similarity of the patterns.

Qualitative spatial gene expression patterns, such as the one shown in Figure 1(a), can be decomposed into a number of basic geometric shapes such as rectangles, disks, and triangles [Figure 1(b)]. For the sake of simplicity, in the following, we will restrict ourselves to a single class of shapes, namely rectangular-shaped components. Still, the same approach can be used for other shapes or combinations of shapes as well.

To allow for reliable recognition of stripes, it is necessary to choose a representation that is invariant against isotropic changes in size, translation (change in position), and rotation. In this way, e.g., when examining stripe formation in *Drosophila melanogaster* [1], formed stripes aligned with the wrong body axis or deviating slightly in size can be detected; promising solutions that could not be identified without the invariants are used in the pattern description. Such an invariant description can be achieved by describing a stripe by a rectangle encompassing the cells that the stripe consists of. To allow for invariance against isotropic changes in size, instead of storing absolute values for breadth, length, and depth, we store the ratio between these three axes; a value staying constant for isotropic transformations. Additionally, since it is not assumed that gene expression domains occur at a specific location in the tissue but rather it is analyzed where an expression domain has formed in the tissue, the description is invariant against translations of domains. Last, since the description of a rectangle by the ratio between its axes ignores the orientation of the rectangle, the description is invariant against rotations. Additionally, by constraining the allowed sizes, recognition of artifacts of small size but correct proportions is avoided.

To identify a stripe in the simulation output, we propose a three-step process:

1) identification of connected cells on the same expression level, later on called connected components (CP). Following the intuition that expression domains formulated in the target patterns are composed of a continuous cell region, we deem CPs a good representation for domains
2) calculation of the principal axis for the identified CPs
3) fitting of the target shape onto the CPs.

Following this scheme (cf. Figure 2 for a schematic overview of the process), first the cells of the model system are assigned to discrete classes according to their expression profile. Using threshold values, the continuous gene-product concentrations [cf. Figure 2(a)] obtained from the tissue model are

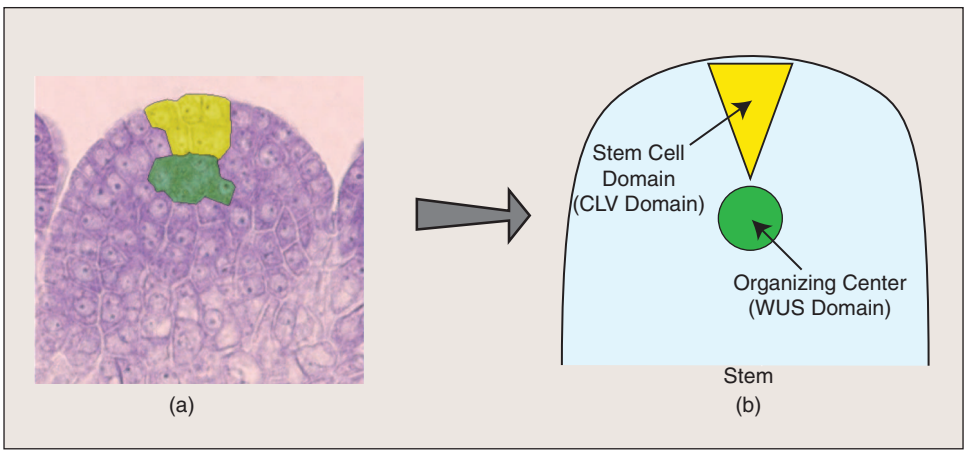

Fig. 1. (a) Microscope image of the SAM, highlighting regions that are important for SAM's maintenance and can be brought in line with specific gene expression patterns; the top-framed region depicts the CLV domain, whereas the lower-framed region in green corresponds to the WUS domain. (b) A sketch of the SAM patterning, derived from the microscope image shown in (a).

The ODEs describe the intracellular interactions between the genes and intercellular interactions between neighboring cells.

discretized [cf. Figure 2(b)]. Afterwards, the sets of connected cells assigned to the same expression class are determined and combined to a CP [cf. blue cells in Figure 2(b)]. For all CPs assigned to genes and expression levels present in the target pattern, their similarity in shape is measured. First, the CP's principal axes [cf. black arrows in Figure 2(b)] are determined by taking the first eigenvectors calculated using a principal component analysis. Starting from a rectangle aligned to the principal axes of the CP and encompassing the whole tissue [cf. outermost rectangle in Figure 2(c)], a greedy heuristic iteratively shrinking the rectangle is applied. First, slices of the tissue are removed for which all cells are not assigned to the CP. Second, the slices are removed for which the difference between cells not assigned to the CP inside the rectangle and cells assigned to the CP outside the rectangle is getting better, i.e., in the considered slice the number of wrong classified cells is larger than the number of right classified cells. Using this procedure, the rectangle is shrunken until no further improvement can be achieved [cf. Figure 2(c)]. Here, it has to be mentioned that the resulting rectangle not necessarily represents the best rectangle with respect to the mentioned cell ratio but provides a reasonably good approximation. Since the systems used in this study only produce stripes parallel to the axis of the rectangular tissue, for this study, the alignment step can be omitted.

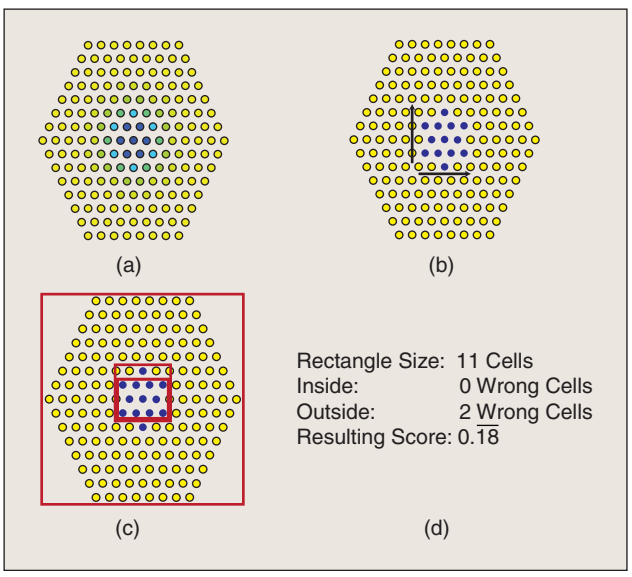

Fig. 2. A schematic overview on the identification and quantification process of the target pattern formed by basic geometric shapes. (a) The distribution of gene-product concentrations over the system, (b) the determined CP and its principal axes, (c) rectangles considered during pattern detection, and (d) the resulting score (see (1)) are shown. In (c), the outermost rectangle represents the rectangle considered when starting the shrinkage process and the inner two rectangles visualize the last step of the shrinkage process. During this last step, only three cells that are located in the bigger of the two rectangles are omitted.

After identifying the rectangle containing the CP, it is checked if the rectangle adheres to the principal axis ratio and if the length and breadth are within the defined intervals. If yes, the scaled difference $g(S_{\text{tissue}})$ between cells correctly classified by the rectangle and those wrongly classified is used to score the similarity between the pattern formed for parameter set x and the target pattern. The similarity score $f_{\text{sim}}(x)$ is given by

$$f_{\text{sim}}(x) = \begin{cases} 1 - g(S_{\text{tissue}}) & \text{if } g(S_{\text{tissue}}) \geq 0, \\ 1 & \text{else.} \end{cases} \quad (1)$$

where

$$g(S_{\text{tissue}}) = \frac{\sum_{i \in S_{\text{rec}}} \mathbf{I}_{S_{\text{CP}}}(i) - \left(\sum_{i \in S_{\text{rec}}} \mathbf{I}_{S_{\text{CP}}^C}(i) + \sum_{i \in S_{\text{rec}}^C} \mathbf{I}_{S_{\text{CP}}}(i) \right)}{|S_{\text{rec}}|}, \quad (2)$$

where the set S_{tissue} denotes all cells in the model, $S_{\text{rec}} \subseteq S_{\text{tissue}}$ refers to all cells within the fitted rectangle (see Figure 2), and $S_{\text{CP}} \subseteq S_{\text{tissue}}$ refers to all cells in the considered CP. S_{rec}^C and S_{CP}^C denote the complements of S_{rec} and S_{CP} with respect to S_{tissue}. The indicator function $\mathbf{I}_S$ is defined as follows:

$$\mathbf{I}_S(i) = \begin{cases} 1 & \text{if } i \in S, \\ 0 & \text{else.} \end{cases}$$

Validation of Proposed Approach

To validate the proposed pattern identification method and similarity measure, we integrated them into the parameter estimation method for spatial multicell GRN models developed by the authors and described in [6]. Then, the resulting algorithm is tested on two GRNs known to be able to form stripes [7], [8].

Parameter Estimation Method

The task of identifying parameters resulting in a specific pattern can be formulated as an optimization problem described by the following design parameters:

- search space $X \subseteq \mathbb{R}^n$ (the n dimensional space of real numbers), where n denotes the number of parameters used for the dynamics equations, and $\mathbb{R}$ represents the set of real numbers
- objective space $Z = \mathbb{R}$
- fitness function $f(x) : \mathbb{R}^n \rightarrow \mathbb{R}$ evaluating the resulting patterns for the given parameters.

For the optimization, we use the covariance matrix adaption evolution strategy (CMA-ES) developed by Hansen and

To allow for reliable recognition of stripes, it is necessary to choose a representation that is invariant against isotropic changes in size, translation, and rotation.

Ostermeier [9]. Evolution strategies are iterative stochastic optimization techniques, developed by Rechenberg [10] and Schwefel [11] in the 60s. Using CMA, during each iteration, new candidate parameter vectors x are generated. They are drawn from a multivariate normal distribution, which is centered around the weighted mean of the previously generated sample vectors. Between the iterations, the covariance matrix of the sample distribution is updated in a way to enlarge the probability to sample a good parameter vector. The CMA-ES has proven its efficiency on several test problems [12] and real-world applications [13].

The fitness function used to build the weighted mean of the parameter vectors generated during an iteration (as it was used in [6]) is designed to capture the formation of general patterns. Three separate aspects are considered: 1) the emerging gene product concentration distribution should stabilize over time; not yet equilibrated, oscillating or diverging systems are penalized; 2) the gene-product concentration distribution throughout the system after simulation should be heterogeneous; and 3) relation between diffusion constants D_{c1}/D_{c2} of specific coupled gene products g_{c1} and g_{c2} are forced to be compliant with a certain threshold δ_D (we use $\delta_D = 0.1$). The fitness function is given by

$$f(x) = \begin{cases} \sum\limits_{i \in \text{gp}} (\max(\delta_\text{t} - \Delta_{s_i}, 0) + \Delta_{t_i}) + \frac{D_{c_1}}{D_{c_2}}, & \text{if } \frac{D_{c_1}}{D_{c_2}} < \delta_D; \\ \sum\limits_{i \in \text{gp}} (\max(\delta_\text{t} - \Delta_{s_i}, 0) + \Delta_{t_i}), & \text{else,} \end{cases} \tag{3}$$

where gp denotes the set of all gene products, and Δ_{si} is the maximal difference in gene product i measured over all cells of the system at the end of the simulation. δ_t is a threshold value, which is used to decide if a given spatial heterogeneity is significant, here $\delta_\text{t} = 0.5$ was used. Δ_{t_i} is the largest change in gene-product concentration i in the last integration step. The first term in the fitness function ($\max(\delta_\text{t} - \Delta_{s_i}, 0)$) can be seen as a penalty term on parameter settings that fail to generate a spatially heterogeneous pattern. In effect, the second term (Δ_{t_i}) penalizes settings for which the simulation does not converge to an equilibrium state within the given number of integration steps.

To not only encompass pattern formation but also pattern similarity, (3) is extended by the similarity grading term given by (1). The resulting fitness function used in this study is given by

$$f(x) = \begin{cases} \sum\limits_{i \in \text{gp}} (\max(\delta_\text{t} - \Delta_{s_i}, 0) + \Delta_{t_i}) + f_\text{sim}(x) + \frac{D_{c_1}}{D_{c_2}}, & \text{if } \frac{D_{c_1}}{D_{c_2}} < \delta_D; \\ \sum\limits_{i \in \text{gp}} (\max(\delta_\text{t} - \Delta_{s_i}, 0) + \Delta_{t_i}) + f_\text{sim}(x), & \text{else.} \end{cases} \tag{4}$$

Test Systems

To evaluate the proposed approach, we used two reaction diffusion (RD) systems [14], which are known to be able to form stripes [7], [8] ([15] explains the biological motivation of the considered systems). The parameters to be estimated are indicated with a hat.

1) An activator [a see (5)] inhibitor [h, see (6)] system in a two-dimensional (2-D) plane composed of 100×10 cells with isotropic diffusion. The plane is initialized with random starting gene-product concentration levels $\text{gp}_i \in [0.0, 0.1]$:

$$\dot{a} = \hat{\rho}_a \frac{a^2}{(1 + \kappa_a a^2)h} - \hat{\mu}_a + \hat{\sigma}_a + \hat{D}_a \Delta a, \tag{5}$$

$$\dot{h} = \hat{\rho}_h a^2 - \hat{\mu}_h h + \hat{\sigma}_h + \hat{D}_h \Delta h, \tag{6}$$

where Δ is the Laplace operator, D_i is the diffusion rate of gene product i, σ_i is a base expression of gene i, μ_i is the degradation rate for gene product i, κ is a saturation constant, and ρ a cross-reaction coefficient [16].

2) An RD system consisting of two independent activator (a_1, a_2) inhibitor (h_1, h_2) systems such as the one described in (5) and (6) in a 2-D plane composed of 30×30 cells with anisotropic diffusion—one of the inhibitors diffuses ten times slower in y direction than in x direction, and the other inhibitor diffuses ten times slower in x direction than in y direction. Additionally, the system uses an effector gene v [4] depending on both activators (a_1, a_2). It is given by

$$\dot{v} = \frac{1}{\tau} g(\sigma v + \rho a_1 + \rho a_2) - \mu_v v, \tag{7}$$

$$g(x) = \frac{1}{2}\left(1 + \frac{x}{\sqrt{1 + x^2}}\right), \tag{8}$$

where τ denotes the inverse maximal rate of gene v, μ_v is the degradation rate of v, and $g(x)$ is a sigmoid function modeling the switch behavior of the response gene. The activator and inhibitor gene-product concentrations for this system are initialized with a linear gradient $\text{gp}_i \in [0.0, 0.1]$; for the first of the two independent systems, the gradient is directed along the x axis with its maximum on the left border and for the second system in y direction with its maximum on the top border. The initial effector gene-product concentrations are set to zero. For (7), the following fixed parameter settings were used: $\tau = 20, \sigma = 0, \rho = 10,$ and $\mu_v = 0.1$.

Results

Because of the stochastic nature of the used parameter estimation method, a set of 12 separate optimization runs was conducted (a detailed list of the identified parameters for each run can be found as supplementary material under http://www.tik.ee.ethz.ch/sop/

Table 1. Stripe describing parameters.

Parameter	Value
Breadth interval	Span 5–15 cells
Length interval	Span 90–100% of one spatial dimension
Considered expression gene	Activator
Considered expression level	Expression > 80% of the minimum adjusted maximal expression after simulation

download/supplementary/parameterEstimation/embmSuppMat.pdf) for both test systems. Each of these runs tested 1,000 parameter vectors and consumed approximately 30 h of computation time on one core of a Dual Core Double CPU AMD Opteron 2.6 GHz 64 b machine with 8GB RAM. During the parameter optimization process, the estimated parameters in (5) and (6) were considered. All runs managed to identify a stripe pattern matching the representation given in Table 1 and, therefore, resulting in a fitness value close to zero. For the first system, the target pattern consisted of one stripe formed by the activator gene, whereas for the second system, each of the independent activator genes had to form a stripe. Since the second system is designed in such a way that one of the activator inhibitor pairs can form vertical stripes whereas the other can form horizontal stripes, the effector gene shows a cross-like pattern or if the stripes are located on the borders of the cell plane, an L-shaped pattern. Since the effector gene v depends on both a_1 and a_2, in the region where both concentrations are high, the cross or L can degenerate to a diamond- or triangular-shaped fraction of a diamond. The resulting patterns for one parameter vector for each test system are shown in Figure 3. Figure 3(a) and (c) shows the relative gene-product concentration distributions obtained for the first- and second test systems, respectively; Figure 3(b) outlines the stripe that was identified using invariant description and pattern identification algorithm on the first system.

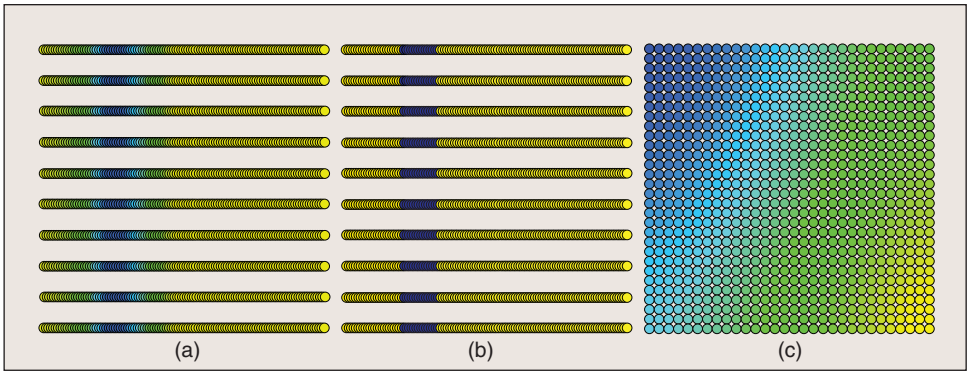

Fig. 3. Example concentration distributions for the considered test systems. For the first test system, (a) shows the gene product concentration distribution obtained during simulation, and (b) illustrates the stripe that was identified for this concentration distribution; (c) depicts the gene-product concentration distribution obtained during simulations for the second system. In the figure, yellow represents low gene-product concentrations and blue represents high concentrations.

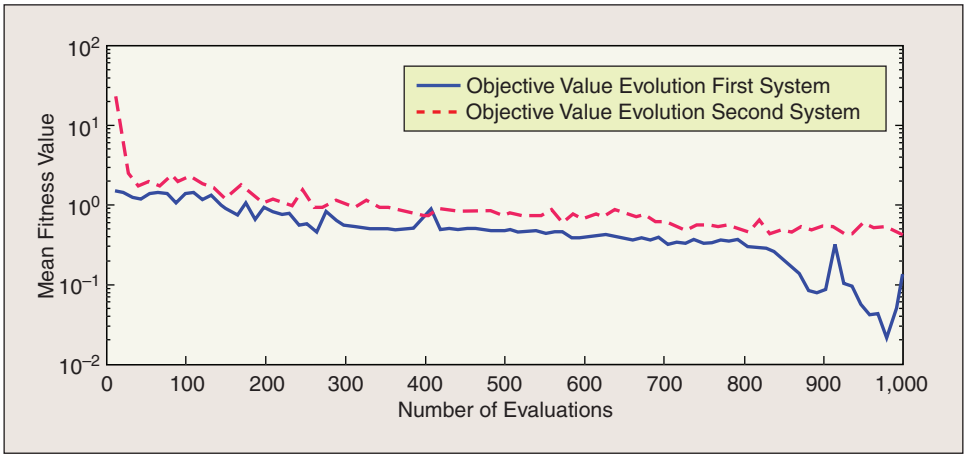

Fig. 4. Time course data about the optimization process for two exemplary runs, one for system (1) and one for system (2), showing a clear trend toward better rated parameter vectors during the minimization process. Plotted are the mean fitness values for the selected offspring parameter vectors generated during one CMA-ES iteration. Worsening in fitness can occur since no elitist strategy is used.

Although the parameter estimation found appropriate parameter vectors for both systems in almost all runs, none of the runs converged to the theoretical optimum of zero [mean fitness in all runs $\mu_f = 0.18$ for system (1) and $\mu_f = 0.367$ for system (2) with a standard deviation of $\sigma_f = 0.23$ for system (1) and $\sigma_f = 0.16$ for system (2)]. The fact that none of the runs converged to zero results from a penalty for not reaching a significance threshold level of $\sigma_f = 0.5$ in (4). Since this threshold was only introduced to make sure that the observed gene product concentration difference is due to the dynamics and does not stem from numerical instabilities in the integration process, the threshold can be lowered in future-fitness functions. Therefore, in effect, the pattern description and similarity scoring worked reasonably well. An exemplary time course of the evolution of the mean fitness of the populations generated during the optimization is shown in Figure 4.

Conclusions

We have presented a formalism to quantify qualitative patterns combined with a method for pattern component identification. Both have been integrated into a parameter estimation

The task of identifying parameters resulting in a specific pattern can be formulated as an optimization problem.

method designed by the authors. This method was applied on two different test systems, aiming at the identification of parameter vectors resulting in stripe-like patterns. For all the tested setups, the proposed method reliably identified parameter sets resulting in the desired target pattern.

Such an approach can be regarded as a first step toward automated network inference for multicell systems using qualitative data only. Even when quantitative data are available, still this method provides a possibility to integrate qualitative data into other inference approaches.

To test the full potential of this method, in the future, other basic geometric shapes will be included as target patterns, and methods will be tested to overlay different shapes to form more complex patterns. Subsequently, the whole setup including parameter estimation and modeling framework will be transferred to three dimensions and applied to patterns and GRNs found in the SAM of *A. thaliana.* It is anticipated that the proposed method can be used for similar applications such as the pattern formation in *D. melanogaster* as well.

In the context of automated hypotheses testing and exploration on spatial gene interaction networks in scenarios where only qualitative data are available, this method provides a necessary first step toward an automated inference method; although this step is crucial for automated hypothesis testing and exploration, still it remains an open question how to adapt the putative GRNs to better explain for the observed patterns.

Acknowledgments

The authors thank Yec'han Laizet for providing the microscope picture used in Figure 1. Tim Hohm has been supported by the European Commission under the Marie Curie Research Training Network SY-STEM, Project 5336.

Tim Hohm received his diploma in computer science in 2003 from the University of Dortmund in Germany. After a two-year stay in the Research Institute Caesar (Bonn, Germany), in 2006, he joined the Systems Optimization Group at Eidgenössische Technische Hochschule (ETH) Zurich headed by Prof. Zitzler. His research focuses on the application of bioinspired optimization techniques on systems biology problems.

Eckart Zitzler received degrees from the University of Dortmund in Germany (diploma in computer science) and ETH Zurich in Switzerland (doctor of technical sciences). Since 2003, he has been an assistant professor for the Systems Optimization Group at the Computer Engineering and Networks Laboratory at the Department of Information Technology and

Electrical Engineering of ETH Zurich, Switzerland. His research focuses on bioinspired computation, multiobjective optimization, computational biology, and computer engineering applications. He was a general cochair of the first three international conferences on evolutionary multicriterion optimization (EMO 2001, EMO 2003, and EMO 2005).

Address for Correspondence: Tim Hohm, Computer Engineering and Networks Laboratory, ETZ G81, Gloriastrasse 35, 8092 Zurich, Switzerland. E-mail: tim.hohm@tik.ee.ethz.ch.

References

[1] E. Knust, "Drosophila morphogenesis: Movement behind the edge," *Curr. Biol.*, vol. 7, no. 9, pp. R558–R561, 1997.
[2] R. Simon, "Function of plant shoot meristems," *Semin. Cell Dev. Biol.*, vol. 12, no. 5, pp. 357–362, 2001.
[3] M. Bansal, V. Belcastro, A. Ambesi-Impiombato, and D. di Bernado, "How to infer gene networks from expression profiles," *Mol. Syst. Biol.*, vol. 3, no. 78, pp. 1–10, 2007.
[4] H. Jönsson, M. Heisler, G. V. Reddy, V. Agrawal, V. Gor, B. E. Shapiro, E. Mjolsness, and E. M. Meyerowitz, "Modeling the organization of the WUSCHEL expression domain in the shoot apical meristem," *Bioinformatics*, vol. 21, Suppl. 1, pp. i232–i240, 2005.
[5] M. Yamaguchi, E. Yoshimoto, and S. Kondo, "Pattern regulation in the stripe of zebrafish suggests an underlying dynamic and autonomous mechanism," *Proc. Nat. Acad. Sci. USA*, vol. 104, no. 12, pp. 4790–4793, 2007.
[6] T. Hohm and E. Zitzler, "Modeling the shoot apical meristem in A. thaliana: Parameter estimation for spatial pattern formation," in *Evolutionary Computation, Machine Learning and Data Mining in Bioinformatics*, (ser. LNCS), E. Marchiori, J. H. Moore, and J. C. Rajapakse, Eds. New York: Springer-Verlag, 2007, vol. 4447, pp. 102–113.
[7] H. Meinhardt and A. Gierer, "Generation and regeneration of sequence and structure during morphogenesis," *J. Theor. Biol.*, vol. 85, no. 3, pp. 429–450, 1980.
[8] A. Gierer, "Generation of biological patterns and form: Some physical, mathematical, and logical aspects," *Prog. Biophys. Mol. Biol.*, vol. 37, no. 1, pp. 1–47, 1982.
[9] N. Hansen and A. Ostermeier, "Adapting arbitrary normal mutation distributions in evolution strategies: The covariance matrix adaptation," in *Proc. IEEE Congress on Evolutionary Computation (CEC 1996)*, Piscataway, NJ, 1996, pp. 312–317.
[10] I. Rechenberg, "Optimierung technischer Systeme nach Prinzipien der biologischen Evolution Dr.-Ing. Dissertation," Verlag Frommann-Holzboog Stuttgart-Bad Cannstatt, Tech. Rep., 1973.
[11] H.-P. Schwefel, *Evolution and Optimum Seeking*. (ser. Sixth-Generation Computer Technology). New York: Wiley, 1995.
[12] A. Auger and N. Hansen, "Performance evaluation of an advanced local search evolutionary algorithm," in *Proc. IEEE Congress on Evolutionary Computation (CEC 2005)*, Piscataway, NJ, 2005, vol. 2, pp. 1777–1784.
[13] C. G. Moles, P. Mendes, and J. R. Banga, "Parameter estimation in biochemical pathways: A comparison of global optimization methods," *Genome Res.*, vol. 13, no. 11, pp. 2467–2474, 2003.
[14] A. Turing, "The chemical basis for morphogenesis," *Philos. Trans. R Soc. Lond. B*, vol. 237, no. 641, pp. 37–72, 1952.
[15] H. Meinhardt, *Models of Biological Pattern Formation*. London, U.K.: Academic, 1982.
[16] A. J. Koch and H. Meinhardt, "Biological pattern formation: From basic mechanisms to complex structures," *Rev. Mod. Phys.*, vol. 66, no. 4, pp. 1481–1510, 1994.